Characterization and Lithographic Parameters Extraction for the Modified Resists

Fu-Hsiang Ko[a], June-Kuen Lu[b], Tieh-Chi Chu[b], Tiao-Yuan Huang[a], Chin-Cheng Yang[a], Jinn-Tsair Sheu[a] and Hui-Ling Huang[c]

[a]National Nano Device Laboratories, National Chiao Tung University, Hsinchu 300, Taiwan
[b]Department of Atomic Science, National Tsing Hua University, Hsinchu 300, Taiwan
[c]Electronics Research & Service Organization, Industrial Technology Research Institute, Chutung Hsinchu 310, Taiwan

ABSTRACT

The modification of the i-line resist structure after spiking with various amount of poly(4-vinylphenol) polymer is characterized by the spectra of ultraviolet visible (UV-VIS) and gel permeation chromatography (GPC). The chemical structure of photoactive compound is found to be unchanged after modification, while slight change in the polymer chain is obserbed. The resist layer coated onto the wafer is characterized by various methods including n&k analyzer, Nanospec, Fourier transform infrared red (FTIR), thermogravimetric analysis (TGA), and differential scanning calorimetry (DSC) to fully evaluate the film properties in terms of porosity, thickness, vibrational spectrum, and thermal stability. Our thermal analysis results show that the resists are mainly decomposed in three stages. The photoactive compound (PAC) is found to decompose during the first stage, while the polymer decomposes during the latter stages. The resist exposure parameters, namely, A, B and C at 365 nm are determined by the absorbance measurement. The extracted parameters are further used in the resist profile simulation by PROLITH/2. It is shown that the spiking of poly(4-vinylphenol) polymer into the resist can improve the resolution and linearity for dense lines. In addition, the swing effects can be reduced by up to 35 and 31 % for dense and isolated lines after resist modification, respectively.

Key words: resist modification; resist characterization; thermal effect; pattern simulation

1. INTRODUCTION

Lithography is one of the most crucial processing steps in semiconductor manufacturing. It is applied repeatedly to the wafer surface for defining the critical device dimensions at different levels, thus affecting significantly not only the device and circuit performance but also the manufacturing cost. Up to date, even the most advanced ULSI manufacturing technologies employ optical lithography for mass production because of its high throughput. In general, a basic lithographic process consists of resist coating, softbake, exposure, post exposure bake, development, and hardbake[1-2], and the resultant pattern profile strongly depends on the resist thickness, baking temperature, baking time, exposure and development conditions. Moreover, different resists, with their various physical and chemical behaviors, greatly affect the lithographic performance especially for deep-submicron design rules[3-4].

The "mix-and-match" technique has received lots of attention in the literatures[5-6]. Due to the higher operation and tool costs for using the KrF stepper, a widely-adopted strategy for technologies employing sub-half micron design rules is to use 248 nm (i.e., KrF) stepper only for the critical levels, while 365 nm (i.e., I-line) stepper is used for all the other non-critical levels. In a lithographic process, the light source first irradiates the resist film, causing optical reaction to occur within the resist. Physical factors including film density, reflectance, and thickness have received extensive attentions due to their distinguishable effects on the resultant patterns. Paniez *et al.* evaluated the influence of film density on the sensitivity, contrast and resolution[7]. Bencher and co-workers[8] reported numerous problems, such as interference, reflective notching and standing waves, associated with proximity effects during exposure. Variations in resist thickness were also known to cause swing and reflective effects.

Despite the emphasis on the physical variations of the film, the chemical effects of resist on lithographic process is as important and of technological interest. This is because the functional groups of the resists may influence the photochemical reaction. Since lithographic performance depends mainly on the chemical structure of the resist, it is important to characterize the chemical composition of the resist. Typical composition of 365 nm (i.e., I-line) resist consists of the casting solvent, photoactive compound (PAC), and polymer. Modification of any component in the resist can effectively change the chemical property, and therefore affect the process window of lithography[9].

Part of the SPIE Conference on Advances in Resist Technology and Processing XVI • Santa Clara, California • March 1999
SPIE Vol. 3678 • 0277-786X/99/$10.00

Downloaded From: http://proceedings.spiedigitallibrary.org/ on 04/28/2014 Terms of Use: http://spiedl.org/terms

However, little has been reported in the literature regarding the effect of polymer modification on the resultant lithographic performance. This could be attributed, at least in part, to the fact that their components in resist are mixture and polymer, therefore structure discrimination is rather difficult. The polymer in the unexposed resist after development and hardbake must be able to withstand the plasma etching and ion implantation. On the other hand, the softbake temperature is of prime importance for lithographic process. This is because too low a softbake temperature may degrade the resist profile due to the mixing of the exposed and unexposed regions by the existing solvent in the layer, while too high a softbake temperature may decompose the PAC, degrading the resist performance as well. The glass transition temperature (Tg) and the thermal decomposition temperature that can be measured by various methods can help to determine the optimum softbake condition[4, 10-11].

In determining the optimum resist exposure procedure, simulation software can help to save significantly the development time[12-14]. Although the basic resist parameters supplied by the vendor can be applied to the simulation software, however, these parameters may differ from those of the real resist used in the manufacturing line. This is because different production lots, purification procedure, transportation and storage condition all can affect the material properties. Therefore, it is important to be able to extract these parameters at the point-of-use for the best simulation results from the simulation software.

This study attempted to investigate the modification of the I-line resist by adding various amounts of polymer, i.e., poly(4-vinylphenol). The variations in chemical structure were then evaluated by Fourier transform infrared red (FTIR), ultraviolet visible (UV-VIS) and gel permeation chromatography (GPC). In addition, thermogravimetric analysis (TGA) and FTIR were also applied to evaluate the thermal effects for the modified resists. The resist samples coated onto the quartz plate were first exposed by a home-made exposure system, and the photo reaction was investigated by the spectrophotometer. After the exposure parameters were extracted, a series of computer simulation was performed to evaluate the modified resists used in lithography.

2. EXPERIMENTAL

2.1 Materials

The positive resist used in this study (i.e., IX850G) was purchased from JSR Company. Modification of resists were prepared by adding 0, 0.25, 0.5 and 1 g of poly(4-vinylphenol) polymer (MW about 8000, Aldrich) into 50 mL resist solution, respectively, and then stirred overnight in a dark room. These resists were named Sample 1 (i.e., non-modified control), 2, 3, and 4 in this work, respectively. Tetrahydrofuran (THF) solvent obtained from E. Merck was used as the diluent (diluted 1: 2500 with THF) for the UV-VIS measurement, and eluted the species in the GPC experiment. The high purity and transparent quartz plates with a dimension of 3 mm thickness by 32 mm diameter were obtained from the ESPI Company.

The relationship between the molecular weight (MW) and retention time for the gel permeation column was calibrated by monitoring the retention time of several pure polystyrene standards including MW of 20650, 10850, 5460, 1050, 580, and 162 Da, respectively. These standards were obtained from Alltech Associates. The total exclusion volume of the GPC system was estimated by using the polyethylene oxide (MW, 1390 KDa). All the polymer standard solutions were prepared with THF solvent and then filtered through the 0.45 μm membrane before use.

2.2 Instrumentation

A dual beam UV-VIS spectrometer (Model U-3300, Hitachi) equipped with quartz cells of 1 cm path length was used to measure the absorbance and electronic spectra of the resist in the range between 190 and 900 nm. The extinction coefficient was calculated with the Beer's law for the modified resists at diluted condition (diluted 1:125000 with THF).

A single-beam UV-VIS spectrophotometer (Spectronic Genesys™ 2PC, Spectronic Instruments) equipped with automatic sampling system was used to measure the absorbance of the resist coated on the quartz plate and the blank sample. The absorbance of the sample with various degrees of exposure by the home-made exposure system was measured at various times.

The GPC system consisted of a dual-piston solvent-delivery pump equipped with an automatic sample injector (Waters 2690). The identification of MW distribution of resist was performed by separating the sample with three columns used in series, namely Styragel™ HR1 (range 100-5K Da), HR2 (range 500-20K Da), and HR3 (range 500-30K Da). The effluent from the column system was detected by the Waters 410 differential refractometer.

The thickness and refractive index of the resist layer were determined by Model 1200 n&k analyzer obtained from n&k Technology, Inc.

Downloaded From: http://proceedings.spiedigitallibrary.org/ on 04/28/2014 Terms of Use: http://spiedl.org/terms

2.3 Sample preparation for thermal analysis

The resist samples were spun onto the wafer and then bake at 105 ℃ by a hotplate for ten minutes. After cooling, the resist film was scrubbed from the wafer and put into the ceramic sample holder of the thermal analyzer (Seiko Model SSC-5200). The sample weight used for thermal analysis was approximately 5 to 10 mg. The heating rate was 10 ℃/min, and the heating cycle was achieved from room temperature to 900 ℃ for the TGA analysis.

The Tg of the various resists was determined by differential scanning calorimetry (DSC) and wafer curvature measurement (WCM). The sample preparation method for DSC method was the same as that of TGA method. The heating rate was 10 ℃/min, and the heating cycle was achieved from –15 to 200 ℃ by an Seiko Model SSC-5200 instrument. WCM was then performed by using Tencor FLX 2320. This method was based on the measurement of the curvature of the wafer from heat induced stress, as described in previous literatures[9, 15].

2.4 Lithographic process and related parameter extraction

Wafers, 6-inch in diameter, were first primed with hexamethyldisilazane (HMDS). They were then coated with various modified resists at various spin rates for 30 sec in order to achieve the same resist thickness. After soft bake (100 degrees, 60 sec), wafers that received various modified resists were sent to film characterization. In order to investigate the variation of sensitivity, contrast and process latitude of the modified resists, samples were exposed with I-line stepper (Hitachi LD-5011iA, Japan). Once exposure the resists were again baked at 120 degrees for 120 sec. Finally, wafers were developed with 2.38 % m/v tetramethylammonium hydroxide (TMAH) using a double puddle process (30/30 sec), and then hard-baked (120 degrees, 120 sec). The resist patterns were examined with the scanning electron microscopy (Hitachi S-6280H).

To perform the parameter extraction, the quartz plate after clean were coated with the modified resists at various spin rates for 30 sec to achieve the same thickness. After soft bake (105 degrees, 60 sec), the samples were sent to film characterization. In order to investigate the exposure parameter, the sample and blank quartz were gone through illumination with the exposure system. The exposure parameters extracted from the above experiment were then used in the simulation software to study the performance of the modified resists in lithography. The simulation program named PROLITH/2 was obtained from FINLE Technologies.

3. RESULTS AND DISCUSSION

3.1 UV-VIS Evaluation and GPC Characterization

In this study, UV-VIS spectrophotometric method was used to evaluate the property of resist after modification. The resist sensitivity parameter in several aspects turns out to be interesting for the lithographic process. The prime consideration is the match between the resist and the energy source of the I-line stepper. The information is provided in the form of a spectral-response curve, which is the measure of the response of the resist with respect to the spectrum of the illumination source. The spectral-response curve as shown in Fig. 1 gives a general indication of the effectiveness of the light source in exposing the resist sample. From this figure it can be seen that Sample 1 (i.e., non-modified control) exhibits strong absorption at wavelength from 200 to 450 nm. Six peaks and shoulders appear at 244, 267, 288, 346, 399 and 423 nm, respectively. Our results also show that all the resists in this study display similar spectra-response curve (data not shown), suggesting similar behavior in terms of electronic absorption. In other words, the resists remain as effective for exposure after modification. The extinction coefficient at 365 nm exposure wavelength are found to be 4875, 4750, 5375 and 4125 for Samples 1 to 4, respectively. These results again suggest that these resists all have the same electronic transition type.

Prior to determining the MW of resists, the molecular weight calibration curve needs to be established based on the polymer standard as mentioned in the experimental section before. The molecular weight range of the three columns used in series is obtained by plotting log (MW) versus elution volume from the columns. It exhibits linear elution behavior for the polymer standards with the MW calibration curve of $y=-0.1839x + 7.4098$, and the correlation coefficient is 0.999. Therefore, the MW of the samples can be easily determined from the elution volume by using the calibration curve.

Fig. 2 shows the chromatograms for the separation of species with various MW in Sample 1 (i.e., non-modified control). It can be seen from the chromatogram that there are a total of 13 peaks to be eluted out. These peaks as estimated from MW calibration curve are found to be at 9756, 4955, 1648, 950, 837, 737, 407, 303, 235, 190, 130, 110, and 89 Da, respectively. The initiation of the first peak is found to be at 30605 Da for Sample 1. The first 6 peaks are believed to be associated with the polymer chain with various MW distributions. The numbers of monomer to be repeated in the peaks of polymers are estimated to be 81, 41, 14, 8, 7 and 6. The peaks attributed to PAC and its related solvent are found to be at

Downloaded From: http://proceedings.spiedigitallibrary.org/ on 04/28/2014 Terms of Use: http://spiedl.org/terms

407, 303 and 235 Da. Furthermore, the other peaks can be attributed to the mixing solvents or the additives.

The chromatograms for other modified resists all depict quite similar peak distribution as in Sample 1, and therefore are not shown here. However, two noticeable differences are found by carefully examining these chromatograms. The first significant difference between Sample 1 and all the other modified samples is the initiation of the first peak. The origin of this peak has been shifted to 42945 Da for all the modified resists, compared to 30605 Da for Sample 1. This variation can be explained by the mechanism that part of the mixing poly (4-vinylphenol) polymerized with the novolak chain, and therefore elutes early from the column system. Another difference is that the peak at 9756 Da for Sample 1 has been shifted to 10618, 11077 and 11077 Da for Samples 2, 3, and 4, respectively. This phenomenon can also be explained by the polymerization of the spiking polymer with the novolak chain of the modified resists. Otherwise, no noticeable shift is observed for all the other polymer peaks. Moreover, the plausible peaks associated with PAC are still eluted at the same time, suggesting that the PAC remains unchanged after resist modification. This finding is compatible with the explanation by using the spectra of UV-VIS prescribed previously and FTIR to be described in the following section.

3.2 FTIR Evaluation

Positive I-line resists are generally composed of three main components: cresol-novolak resin, PAC, and organic solvent. PAC changes to indene ketene by exposure to 365 nm light source, and subsequently reacts with water to form the indene carboxylic acid[16]. To characterize the resist after modification, FTIR spectrum is a simple method for revealing the structure conversion after spiking polymer. Fig. 3 shows FTIR spectra for various samples. The absorption peak appeared at 3406 cm^{-1} for Curve a (Sample 1) in Fig. 3 can be attributed to the stretching vibration of the hydroxyl group grafted on polymer chain. Since a typical free hydroxyl bond exhibits[17] a sharp peak in the range 3590-3650 cm^{-1}, the broad absorption within range 3200-3500 cm^{-1} can be attributed to the formation of intermolecular hydrogen bond between polymer and PAC. Based on the bonding property, the electron of the hydroxyl bond on the polymer by PAC can be delocalized, and therefore decreases the bond vibration frequency. The magnitude of the shift of the vibration mode can be used to reveal the extent of hydrogen bonding.

By examining Curves a to d for Samples 1 to 4, respectively, it is noticed that while the stretching vibration remains unchanged at 3406 cm^{-1} for Curves a to c (Samples 1 to 3), this peak shifts to 3400 cm^{-1} for Curve d (Sample 4). The red shift of the vibration mode found in Sample 4 is due to the stronger hydrogen bond by intermolecular interaction. It can be deduced that the addition of poly(4-vinylphenol) facilitates the intermolecular hydrogen bonding. Therefore, the vibration frequency of hydroxyl group on polymer is reduced by the addition of sufficient polymer. Another peak associated with the variation of hydroxyl bond can be identified by the absorption of in-plane bending vibration mode near 1470 cm^{-1} for Curve a (Sample 1), while a distinguishable shoulder peak appeared at 1454 cm^{-1} for Curves b to d (Samples 2 to 4). The lower bending mode found in the modified resists also reflects the higher hydrogen bonding by the spiking polymer.

Previously, Norbury *et al.* has demonstrated the two models between the PAC and the polymer [18]. In the first model, the PAC is free in the resist solution. While in the second model, the PAC is permanently bonded to the polymer by using a capping technology. In this work, the two peaks found at 1713 and 1600 cm^{-1} in Curve a of Fig. 3 represent the various degrees of bonding between polymer and PAC. According to the first model, the carbonyl group of free PAC can be found at higher vibration mode of 1713 cm^{-1}. In addition, the electron delocalization of the carbonyl group shifts the vibrational absorption to 1600 cm^{-1} by the hydrogen bonding. The above result indicates that the PAC can exist in the resist layer in either free state or binding interaction. By reviewing the spectra from Curves b to d of Fig. 3, the apparent shoulder peaks are found near 1713 and 1600 cm^{-1}, however, the main peak position at 1713 and 1600 cm^{-1} remains unchanged. The shoulder peaks can be explained by the fact that the addition of poly(4-vinylphenol) further exerts hydrogen bonding on part of the PAC.

Due to the photo-sensitive feature of PAC, it is important to understand the variation of the PAC after resist modification. The most useful method to determine the extent of PAC conversion can be obtained from the vibration mode of diazo group[3]. Fig. 3 clearly shows that the vibration doublet of diazo peaks appear at 2164 and 2118 cm^{-1}. The position and the absorption ratio of the two respective peaks are kept constant for all the samples, which indicate that the chemical structure of PAC is unchanged after modification. This finding is also consistent with the UV-VIS and GPC methods to be discussed in the preceding section.

3.3 Thermal Analysis

In lithographic process, it is required to process the wafer after resist coating through various thermal processes, i.e., softbake, post exposure bake and hardbake. The thermal process window is strongly dependent on the resist structure. Generally, positive resist shows endothermic reaction due to thermally induced decomposition, while the negative resist shows exothermic reaction due to thermally induced crosslinking[4]. The thermal stability of the resist can be evaluated by

Downloaded From: http://proceedings.spiedigitallibrary.org/ on 04/28/2014 Terms of Use: http://spiedl.org/terms

methods of TGA and DSC, and consequently, the reaction heat type and Tg can be determined. These results can help determine the range of baking temperature and maximum allowable softbake temperature in semiconductor manufacturing process.

Fig. 4 shows the effect of elevating the baking temperature on the percentage of remaining weight and the first derivative of weight variation from the TGA method. It can be seen that the resist weight loss increases with increasing temperature. From the first derivative in this figure, three distinctive peaks are observed at 142, 357 and 509 ℃, respectively. The obvious three-stage weight loss in the TGA curve is estimated to be 6, 21 and 12 %, respectively. It is interesting to note that there still exists about 30 % of resist residual even after baking at 900 ℃. To resolve which ingredients in the resist cause weight loss at each stage, the FTIR spectrum was performed. The FTIR results show that the two vibrational peaks are found at 2118 and 2164 cm^{-1}, respectively. The vibrational doublet peaks can be assigned to the diazo group in the photoactive compound of resist. The tendency of decreasing the peak height with increasing baking temperature can be attributed to the thermal destruction of photoactive compound. It should be noted that no appreciable peaks occur at baking temperature up to 180 ℃. Although not shown here, the characteristic peaks appeared at 1713 and 1600 cm^{-1} are stable up to 180 ℃. This illustrates that the polymer in all the samples does not decompose at the first stage.

The above evidence suggests that the weight loss at Peak I in Fig. 4 can be explained by the thermal decomposition of photoactive compound. Furthermore, the temperature at which Peak I occurs suggests that the softbake temperature of Sample 1 should be properly operated at a temperature lower than 107 ℃. Peaks II and III at higher temperature (i.e., 357 and 509 ℃) are most likely associated with the thermally induced polymer degradation effect. Since all modified resists depict similar TGA and FTIR spectra as those found in Sample 1, indicating that the resist modification with poly (4-vinylphenol) polymer has no significant effects on the thermal property of resists. Therefore, the process window of baking temperature for all the resist samples should be similar.

In addition to the above-mentioned thermal evaluation by TGA, DSC is also a useful technique. DSC method can evaluate the temperature effect and the heat exchange associated with transitions in materials, therefore the Tg value can be easily determined from the heating curve. Schiltz and Paniez[9] have demonstrated another method, namely WCM, to obtain the Tg value from the stress measurement. The WCM method progressively monitors the curvature of the resist-coated wafer at a heating rate 10 ℃/min. The stress variations induce the wafer bending at higher temperature, and subsequently, the bending curvature of the wafer is determined by the in-line optical method.

In this study, both DSC and WCM methods were used to determine the resists' Tg value. Table 1 summarizes the Tg results. It can be seen that all Tg values fall within the range between 85 and 95 ℃, as verified by the two independent Tg measurement methods. The fact that resists after spiking with various amounts of poly (4-vinyphenol) polymer display similar Tg value suggests that the thermal property of the resist can not be changed by only polymer modification.

3.4 Lithographic parameter extraction and Simulation Study

The absorption of light by the photoactive compound in positive resist can be used as an indicator for the evaluation of the extents of photo reaction. To describe the behavior of resist's photo reaction, Dill et al. first proposed the equations for exposure parameters A, B and C in 1975[19-20]. They successfully derived the basic equation of parameters A, B and C from the Lambert-Beer law, which leads to a set of asymptotic relationship based on the transmittance (T(0)) of resist film at the beginning of exposure, the initial rate of change of transmittance (dT(0)/dt), and the transmittance ($T(\infty)$) after full exposure. The equation of parameters A, B and C in the resist film with specific thickness (d) is listed in the following:

$$A = \frac{1}{d} \cdot \ln \frac{T(\infty)}{T(0)}$$

$$B = -\frac{1}{d} \cdot \ln T(\infty)$$

$$C = \frac{A+B}{A I_0 T(0)(1-T(0))} \cdot \frac{dT(0)}{dt}$$

where parameter A denotes the light absorbed by the photoactive compound, B represents the light absorbed by the polymer, and C is the decomposition rate of photoactive compound. I_0 is the light intensity at the surface of the resist film.

Basically, these parameters can be extracted from the experimental method based on the relationship of transmittance and exposure dose, and can further be utilized in the lithographic profile simulation. In this study, various modified I-line resists were first coated onto different quartz substrates. The substrates were then exposed with a home-made illumination

Downloaded From: http://proceedings.spiedigitallibrary.org/ on 04/28/2014 Terms of Use: http://spiedl.org/terms

system. Samples were then sent to the UV-VIS spectrophotometer for absorbance measurement. Afterwards, samples were again exposed with the 365 nm light and the absorbance was determined by UV-VIS. The exposure process and absorbance measurements were repeatedly operated until the photoactive compound was fully bleached out.

Fig. 5 shows the effect of exposure dose on the transmittance of the resists. It can be seen that the transmittance increases linearly from about 0.5 at initial exposure to near 0.75 with exposure energy of 98 mJ/cm^2, and then slowly increases to 0.82 at an energy of 186 mJ/cm^2 for all samples. Beyond that, the transmittance levels off up to the exposure dose of 588 mJ/cm^2. This indicates that the PAC gradually decomposes by exposure with 365 nm light source, therefore the transmittance increases. However, the resist reaches the bleach-out state before the PAC can be fully decomposed into indene carboxylic acid, thus the transmittance is retained.

Table 2 summarizes the results of thickness, refractive index and parameters A, B, and C for the various resist layers. The difference in all the parameters appeared in this table can be attributed to the resist modification. The resist structure after modification has been discussed in previous section. Regarding the exposure parameters A, B, and C, it can be seen that only parameter A increases with increasing amount of spiking polymer.

In lithographic study, patterns of dense and isolated lines are often used to evaluate the behavior. Dense lines are defined as the same critical dimension (CD) for line and space, while isolated lines are defined as a CD ratio between space and line of larger than 10. Simulations were carried out by PROLITH/2 software for both the isolated and dense line patterns with parameters A, B, and C extracted from previous sections. Fig. 6 shows the effects of nominal mask linewidth on resist linewidth with a len with 0.42 numerical aperture and 0.5 coherence factor. As can be seen from Fig. 6a, the isolated lines possess a linear relationship between 0.3 and 1.2 μm for all the modified resists, while the control sample reaches a plateau at nominal linewidth lower than 0.4 μm. On the other hand, the dense lines behave quite differently. As shown in Fig. 6b, the resist CD depicts a minimum value of about 0.5, 0.48, 0.45 and 0.48 μm for Samples 1 to 4, respectively. The following question then arises: Why should the dense lines behave so differently as compared with isolated lines. As explained by Huygen's principle, based on the optical interference effect, denser mask patterns lead to larger diffraction angle under the same illumination wavelength. Since the image behind the mask can not be fully collected by the projection len, a smaller feature size can not be achieved for the denser mask patterns. According to the simulation results for dense lines, the modified resist of Sample 3 has wider linearity as compared with others. This suggests that spiking an optimum amount of poly(4-vinylphenol) polymer can improve the pattern performance for dense lines.

In order to investigate the effects of parameters A, B, and C on the resist linewidth, a series of simulation was carried out to clarify the resist performance for future development on the functional resist. Figs. 7 and 8 depict the effects of nominal mask linewidth on resist linewidth for isolated and dense patterns, respectively. Figs. 7a and 7b demonstrate that increasing the parameters A and B for a specific mask linewidth can deteriorate the resist linewidth for isolated lines. However, Fig. 7c shows that parameter C depicts the opposite trend, i.e., increasing the parameter C can improve the resist resolution limit for isolated lines. As shown in Figs. 8a and 8b, increasing parameters A and B may degrade the linearity and resolution limit for the dense lines. In contrast, Fig. 8c indicates that increasing the parameter C should improve both the linearity and resist pattern resolution.

The interference effect of resist film comes from the exposure with various amounts of dose can be represented by a swing curve[12, 14]. Generally, to characterize the swing effect, a number of wafers are coated with increasing thickness of resist and gone through the light illumination. The dose to clear is measured as the minimum energy required to clear the exposure field after resist development. Fig. 9 depicts the typical swing curve. The maximums of the swing curve indicate that destructive interference occurs at a specific thickness, and here more energy is required to fully expose the resist. Conversely, at either side of these maximums a regime of constructive interference occurs and less energy is required to fully expose the resist.

PROLITH/2 software can also be used to simulate the effect of resist thickness on resist linewidth to replace the time-consuming experiments. In this simulation software, the value of swing ratio (SR) is defined in the following:

$$SR = 2 \cdot \frac{(LW_{max} - LW_{min})}{(LW_{max} + LW_{min})} \cdot 100\%$$

Where LW_{max} represents the average line width of the first two maximums, and LW_{min} is the linewidth at the minimum between these two maximums.

Table 3 shows the simulation results of swing ratio for 0.5μm nominal dense and isolated lines. It is interesting to find that the swing ratio of the dense lines is higher than that of the isolated lines. More importantly, the swing ratio decreases by increasing the spiking amount of polymer into the resist, especially in the case of isolated lines. The primary benefits of reducing swing effect are to enhance the focus/exposure latitude and linewidth control in lithography. Previously, it has been known that the addition of either a top or bottom anti-reflective layer can reduce the swing effect[8, 21-23]. In this paper we

Downloaded From: http://proceedings.spiedigitallibrary.org/ on 04/28/2014 Terms of Use: http://spiedl.org/terms

show, for the first time that the swing ratio can also be reduced by up to 35 and 31 % for the dense and isolated lines, respectively, by simply modifying a commercial resist. According to our previous data[24], spiking polymer can only change the molecular weight distribution of the polymer chain, and has no effect on photoactive compound. Therefore, the reducing of swing effect is attributed to the polymer modification. Our approach thus offers an alternative way to improve the swing effect for future development of functional resists.

4. CONCLUSIONS

In this work, we have studied the structural variations of modified resist obtained by adding poly(4-vinylphenol) polymer. Spectroscopic results from UV-VIS, GPC and FTIR were employed for analysis. The chemical structure of photoactive compound is found to be unchanged after modification, while a slight structure change is observed in the polymer chain. The maximum allowable softbake temperature for the resist coated onto the wafer have been determined to be 107 ℃ by the TGA method. The thermal stability of the resist, as evaluated by the first derivative of the TGA curve and the FTIR method, shows that the first thermal decomposition in the TGA curve is attributed to the PAC destruction, and that at the other two stages is attributed to the polymer degradation. The Dill's parameters obtained from the photochemical reaction are then used in the PROLITH/2 simulation software. Our simulation results show that the resolution limit and the linearity of the resists with respective to the mask linewidth are improved by the spiking polymer. The reduction of swing effect for the resist after polymer modification may be explained by the elimination of substrate reflectivity due to the polymerization reaction between poly(4-vinylphenol) and the novolak polymer. Our approach thus offers a simple way to improve the swing effect for the resists.

ACKNOWLEDGMENTS

The authors would like to thank the National Science Council of Taiwan, R.O.C., for supporting this research through contract #NSC88-2721-2317-100.

REFERENCES

1. C. Y. Chang, and S. M. Sze, *ULSI Technology*, McGRAW-HILL, NY, 1996.
2. W. M. Moreau, *Semiconductor Lithography*, Plenum, NY, 1991.
3. E. Fadda, C. Clarisse, and P. J. Paniez, *Microelec. Eng.*, **30**, pp.593, 1996.
4. E. Tegou, E. Gogolides, and M. Hatzakis, *Microelec. Eng.*, **35**, pp.141, 1997.
5. J. Greeneich, *Solid State Technology*, Oct., pp.79, 1994.
6. M. O. Levenson, *Solid State Technology*, Apr., pp.34, 1995.
7. P. J. Paniez, G. Festes, and J-P. Chollet, *Proc. SPIE*, **1672**, pp.623, 1992.
8. C. Bencher, C. Ngai, B. Roman, S. Lian, and T., Vuong, *Solid State Technol.*, **40-3**, pp.109, 1997.
9. A. Schiltz, and P. J. Paniez, *Microelec. Eng.*, **27**, pp.413, 1995.
10. E. Gogolides, and M. Hatzakis, *Microelectric. Eng.*, **30**, pp.267, 1996.
11. A. Schiltz, J. F. Terpan, S. Brun, and P. J. Paniez, *Microelec. Eng.*, **30**, pp.283, 1996.
12. J. Lamb, and M. G. Moss, *Solid State Technology*, Sep., pp.79, 1993.
13. A. Sekiguchi, C. A. Mack, Y. Minami, and T. Matsuzawa, *Proc. SPIE*, **2725**, pp.49, 1996.
14. B. Martin, and G. Arthur, *Microelec. Eng.*, **30**, pp.153, 1996.
15. P. A. Flinn, *J. Mat. Res.*, **6**, pp.41, 1991.
16. A. Sekiguchi, Y. Minami, T. Matsuzawa, T. Takezawa, and H. Miyakawa, *Electronics and Communications in Japan*, **78**, pp.21, 1995.
17. E. Pretsch, J. Seibl, and T. Clerc, Spectra Data for Structure Determination of Organic Compounds, Springer-Verlag, Berlin Germany, 1983.
18. D. H. Norbury, and J. C. Love, *Proc. SPIE*, **1463**, pp.558, 1991.
19. F. H. Dill, W. P. Hornberger, P. S. Hauge, and J. M. Shaw, *IEEE Trans. Electron Devices*, **22**, pp.445, 1975.
20. F. H. Dill, A. K. Neureuther, J. A. Tuttle, and E. J. Walker, *IEEE Trans Electron Devices*, **22**, pp.456, 1975.
21. Tanaka, T., Hasegawa, N., Shiraishi, H. and Okazaki, S., *J. Electrochem. Soc.*, **137**, pp.3900, 1990.
22. T. Perera, *Solid State Technology*, Jul., pp.131, 1995.
23. J. Strutevant, and B. Roman, *Microlithography World*, Aut., pp.13, 1995.
24. F.-H. Ko, C.-S. Wu, H.-L. Huang, T.-C. Chu, H.-A. Chang, B.-J. Cheng, and M. Yang, *Proceedings of the Fifth Symposium on Nano Device Technolgy*, pp.174, 1998.

Downloaded From: http://proceedings.spiedigitallibrary.org/ on 04/28/2014 Terms of Use: http://spiedl.org/terms

Table 1. Glass transition temperature (Tg) of various resists

Tg, ℃	Sample 1	Sample 2	Sample 3	Sample 4
DSC	85	86	87	89
WCM	88	92	90	95

Table 2. Thickness, refractive index, and exposure parameters for various resists

	thickness, μm	refractive index	A	B	C
Sample 1	0.927	1.694	0.5156	0.1761	0.00986
Sample 2	0.99	1.697	0.5701	0.1939	0.0142
Sample 3	1.03	1.692	0.5933	0.1973	0.0131
Sample 4	1.153	1.692	0.6667	0.1543	0.0151

Table 3. Resists swing ratio for 0.5 μm dense and isolated lines

	dense line, %	isolated line, %
Sample 1	59.9	37.6
Sample 2	40.9	27.1
Sample 3	42.7	27.0
Sample 4	38.8	26.1

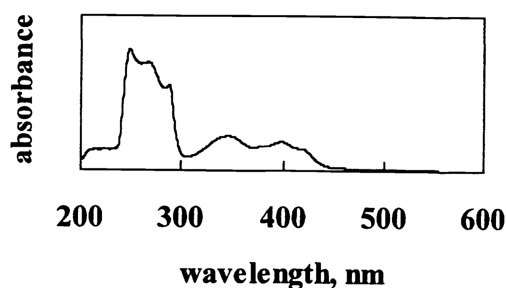

Fig. 1. Ultraviolet-visible (UV-VIS) absorption spectra of Sample 1 (1:2500 dilution).

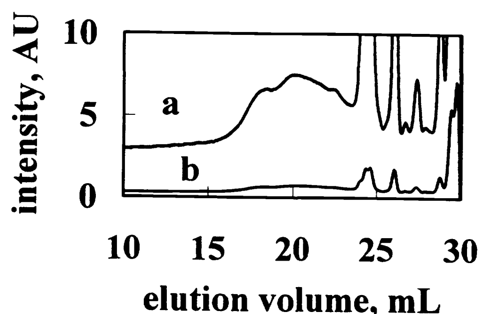

Fig. 2. Chromatograms obtained by the gel permeation chromatography (GPC) method for (a). Sample 1, and (b). intensity of Sample 1 after 10-fold reduction. Column: Waters Styragel™ HR1, HR 2 and HR 3; mobile phase: THF; flow rate: 1 mL/min; sample size: 100 μL.

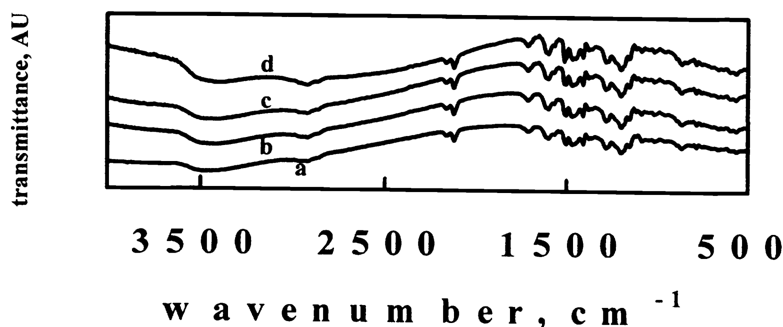

Fig. 3. FTIR absorption spectra. Curves a, b, c, d, are for Samples 1, 2, 3, 4, respectively.

Downloaded From: http://proceedings.spiedigitallibrary.org/ on 04/28/2014 Terms of Use: http://spiedl.org/terms

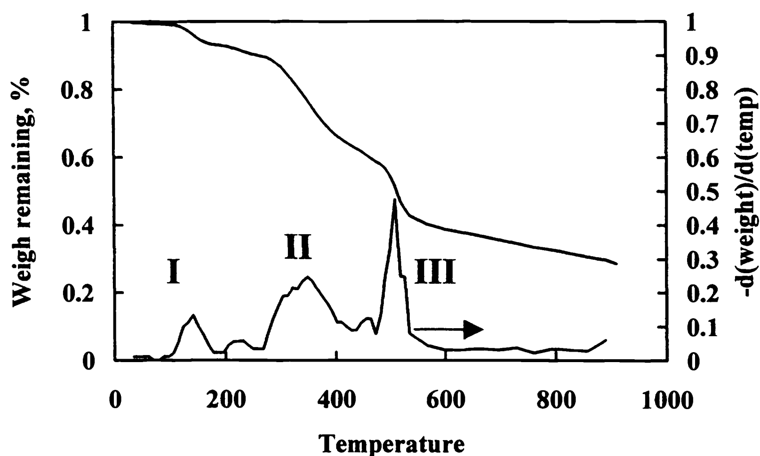

Fig. 4. Weight variation of Sample 1 determined by thermogravimetric analysis (TGA) method.

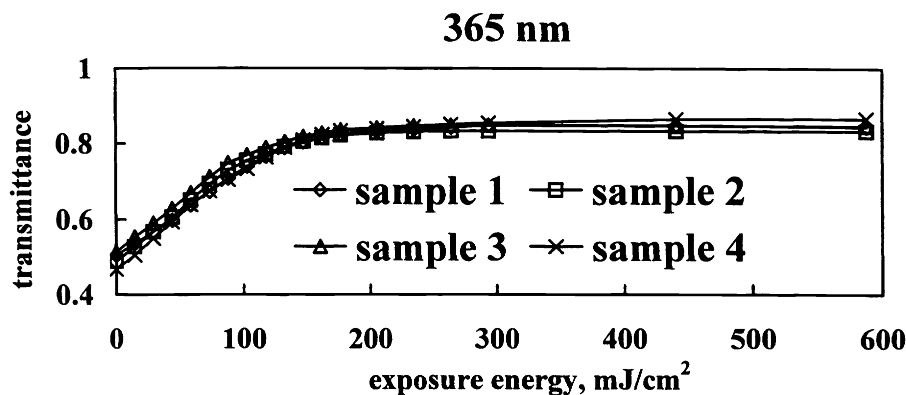

Fig. 5. Effect of exposure energy on the transmittance for various resist samples.

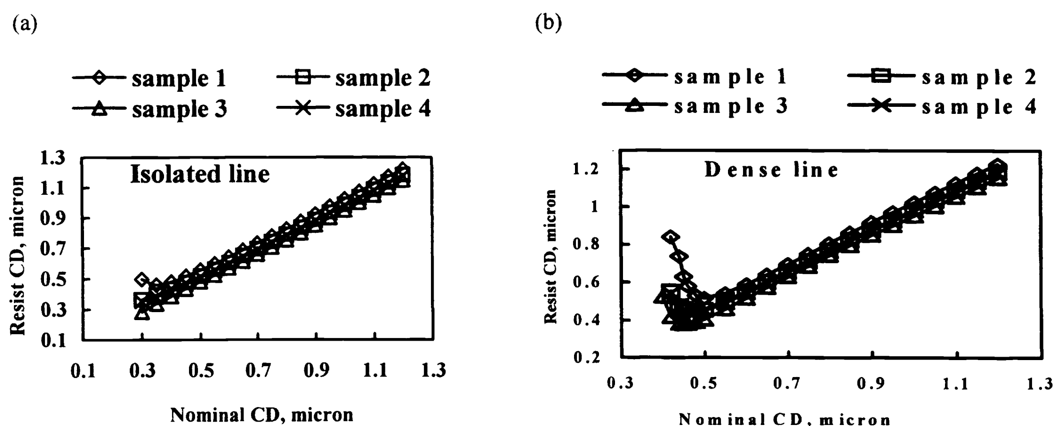

Fig. 6. Resist linewidth as a function of nominal mask linewidth for (a). isolated and (b). dense lines.

Downloaded From: http://proceedings.spiedigitallibrary.org/ on 04/28/2014 Terms of Use: http://spiedl.org/terms

(a)

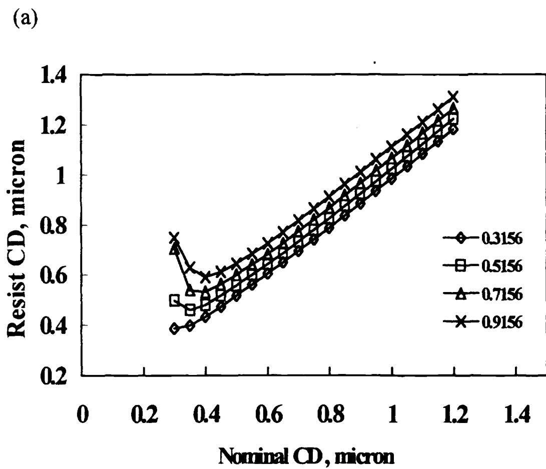

(a)

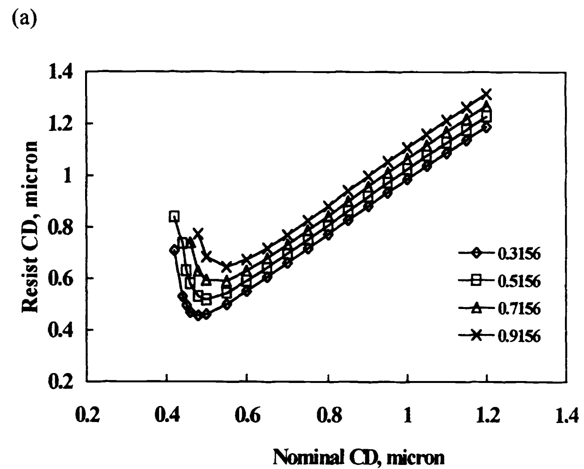

(b)

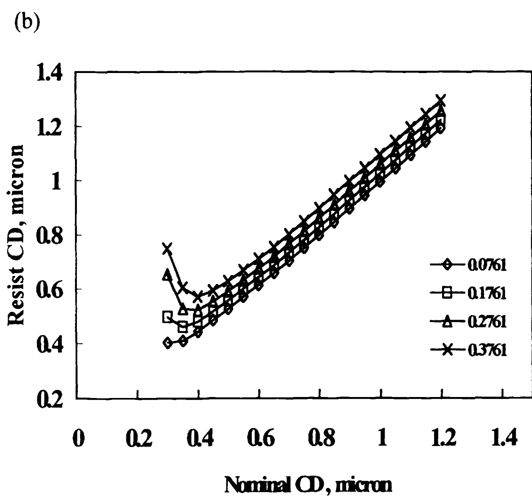

(b)

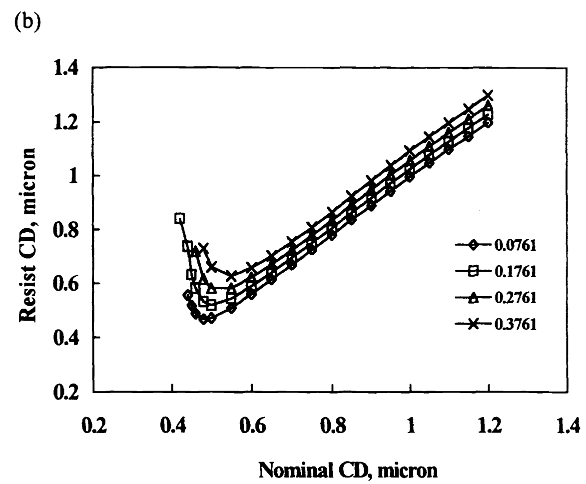

(c)

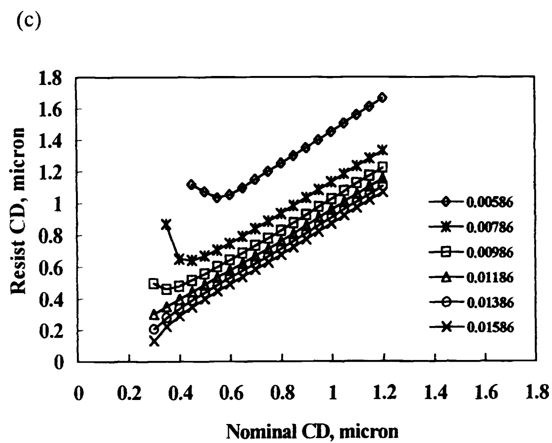

(c)

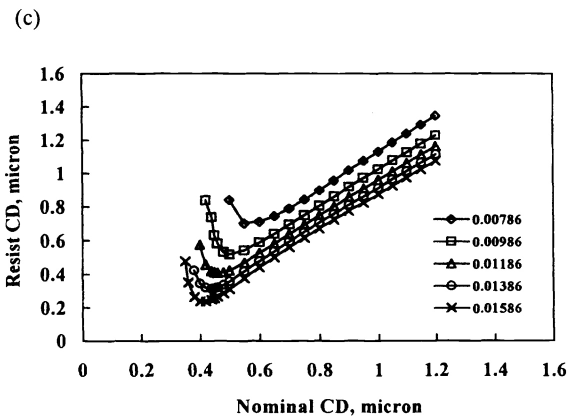

Fig. 7. Resist linewidth as a function of nominal mask linewidth for isolated lines with various exposure (a). A, (b). B, and (c). C parameters.

Fig. 8. Resist linewidth as a function of nominal mask linewidth for dense lines with various exposure (a). A, (b). B, and (c). C parameters.

Downloaded From: http://proceedings.spiedigitallibrary.org/ on 04/28/2014 Terms of Use: http://spiedl.org/terms

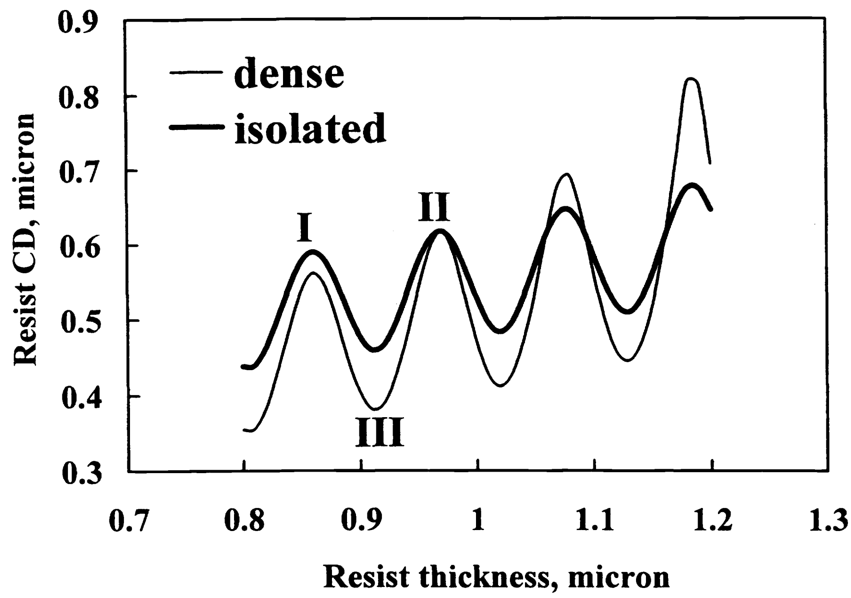

Fig. 9. Typical swing curves for the resist.

Downloaded From: http://proceedings.spiedigitallibrary.org/ on 04/28/2014 Terms of Use: http://spiedl.org/terms